



Preparation and characterization of self-standing and flexible CuS/rGO composite paper

Ezgi Topçu* , Kader Dağcı Kıranşan 

Atatürk University, Faculty of Science, Department of Chemistry, 25240, Erzurum, Turkey

Abstract

A self-standing, durable, and flexible CuS/reduced graphene oxide (rGO) composite paper electrode was synthesized through a facile electrochemical deposition of CuS on the surface of the rGO paper. CuS/rGO composite paper electrode was characterized by using X-ray photoelectron spectroscopy (XPS), X-ray diffraction (XRD), scanning electron microscopy (SEM), and Raman spectroscopy. The morphological characterization displayed that the surface of the rGO paper electrode was covered with ball-like CuS structures. Microstructures of rGO and CuS/rGO papers and the intensity of surface defects were compared with Raman spectra. Electrochemical studies exhibited that as-prepared flexible CuS/rGO composite paper electrode has very high electrochemical activity.

Keywords: CuS, graphene-based electrode, characterization

1. Introduction

Graphene papers are generally used to obtain flexible electrodes [1-3]. These materials, due to possessing cuttable, rollable, and shapeable features, have attracted more interest in many areas such as hydrogen-oxygen evolution reactions [4], lithium-ion batteries [5], supercapacitors [6], and sensors [7-9]. Recent studies have shown that flexible graphene papers display excellent chemical, mechanical, and physical features such as high mechanical strength, high electrical conductivity, chemical stability, and flexibility [10,11].


Graphene papers can be modified with various materials to prepare composite graphene-based papers, resulting in improving mechanical, electrical, and chemical properties of the graphene-based papers [12,13]. In this regard, modification of the graphene surfaces with semiconductor metal chalcogenides attracts attention in recent years [14,15].

Among the different semiconductors, the covellite phase copper monosulfide (CuS) is the most important metal chalcogenide, which is of great interest with its modern applications ranging from biomedical to industrial and its structural, optical, and surface properties, which are very different from

the bulk material due to its superior chemical and physical properties. CuS is a non-toxic p-type semiconductor having a direct band gap [14]. The importance of CuS in semiconductor materials is high conductivity, excellent metallic properties, and convertibility to superconductors at about 1.6K [16]. CuS nanostructures have been synthesized by various methods such as chemical co-precipitation method [17], hydrothermal or solvothermal methods [18,19], solid-state reaction method [20] and sonochemical method [21] over the years.

In this study, CuS structures synthesized through a simple hydrothermal method were coated on the rGO paper electrode surface by using the electrochemical technique. The morphological and structural analysis of CuS/rGO composite paper was characterized by using XPS, XRD, SEM, and Raman spectroscopy, and the electrochemical performance of this composite paper was investigated by using CV and EIS techniques. The results of the characterization studies showed that self-standing CuS/rGO composite paper was successfully prepared and its electrochemical activity was high enough to be used as an electrode

Citation: E. Topçu, K. Dağcı Kıranşan, Preparation and characterization of self-standing and flexible CuS/rGO composite paper, Turk J Anal Chem, 2(1), 2020, 1-6.

 <https://doi.org/>

***Author of correspondence:** ezgitopcu@atauni.edu.tr

Phone: +90 (442) 231 44 07, **Fax:** +90 (442)231 41 09

Received: April 09, 2020

Accepted: May 04, 2020

2. Experimental section

2.1. Preparation of rGO paper

Modified Hummer's method was used to synthesize GO [22]. 100 mL of the GO (1.0 mg mL^{-1}) suspension was filtrated through a nucleopore polycarbonate membrane filter (Whatman; $\varnothing=47 \text{ mm}$; pore size, $0.2 \mu\text{m}$) by using ultrafiltration vacuum cell. To obtain GO paper, this process is followed by washing, air drying, and peeling off from the filter. GO paper was immersed in a HI solution for 1 h to fabricate rGO paper. The rGO paper was washed with copious ethanol and distilled water and dried in air. This conductive rGO paper, prepared with a radius of approximately 47 mm each time, was cut into a strip shape ($25 \text{ mm} \times 5 \text{ mm}$) and directly used as an electrode in the electrochemical studies.

2.2. Synthesis of CuS crystals

Copper (II) sulfate pentahydrate ($\text{CuSO}_4 \cdot 5\text{H}_2\text{O}$) and sodium sulfide nonahydrate ($\text{Na}_2\text{S} \cdot 9\text{H}_2\text{O}$) were used as precursors and L-cysteine ($\text{C}_3\text{H}_7\text{NO}_2\text{S}$) was used as a surface ligand [23]. The distilled water as the solvent was used to prepare all solutions. 5 ml of 0.1 M $\text{CuSO}_4 \cdot 5\text{H}_2\text{O}$ and 20 mL of 0.1 M $\text{C}_3\text{H}_7\text{NO}_2\text{S}$ were mixed. The pH of the solution was adjusted to 11 with 2 M NaOH. 5.0 ml of 0.1 M $\text{Na}_2\text{S} \cdot 9\text{H}_2\text{O}$ was added to this solution. The mixture was then refluxed and stirred at 95°C . The solution heated for 4 h before it was cooled down to room temperature. The formed precipitates were collected and washed with ethanol several times before it was dried at 60°C in the air [23].

2.3. Electrochemical fabrication of CuS/rGO composite paper

CuS dispersion was prepared through the ultrasonic treatment of the mixture of CuS powder, and 0.1 M NaNO_3 containing dimethylformamide (DMF: $\text{C}_3\text{H}_7\text{NO}$) and 0.05 M NaOH solutions. The electrodeposition of CuS on the surface of rGO paper was performed by applying cyclic voltammetry from 0 to -1200 mV potentials in a suspension of 5 mM CuS. The obtained paper was denoted as CuS/rGO.

2.4. Characterization

Scanning electron microscopy (SEM) images were performed by using SEM, ZEISS SIGMA 300 for the morphological investigations, equipped to the elemental analysis by energy-dispersive X-ray spectroscopy (EDS). The surface chemical composition was studied by X-ray photoelectron spectroscopy (XPS) using Spect-Flex with standart Al

X-ray source. Material characterization was acquired using the Rigaku TTR III X-ray diffractometer (XRD) with monochromatized $\text{Cu K}\alpha$ radiation ($\lambda=1.5406 \text{ \AA}$). A micro-Raman spectrometer (WITech alpha 300R) was used to record Raman spectra under atmospheric conditions.

2.5. Electrochemical performance of composite paper electrode

In the three-electrode system, a strip of rGO paper was directly used as the working electrode, platinum wire and Ag/AgCl (saturated KCl) (BASi) electrode were used as counter and reference electrodes, respectively. Cyclic voltammetry (CV), and electrochemical impedance spectroscopy (EIS) tests were performed with Gamry (600+) potentiostat system. The EIS were investigated over the frequency range from 0.1 to $1 \times 10^5 \text{ Hz}$ at the open circuit potential by using an AC voltage of 5 mV.

3. Results and discussion

The schematic of the fabrication of flexible CuS/rGO composite paper was shown in Fig. 1. rGO paper was prepared in two steps. Firstly, GO dispersion was filtrated through a simple vacuum filtration system to obtain GO paper. Then, GO paper was chemically reduced by immersing it into HI solution to provide conductivity and converted to rGO paper. This rGO paper was cut into a rectangular strip and directly used as a working electrode in the electrochemical system. rGO paper electrode surface was electrochemically coated with the CuS structure in the solution containing CuS, thus self-standing and flexible CuS/rGO paper electrode was successfully prepared in this way (Fig. 1).

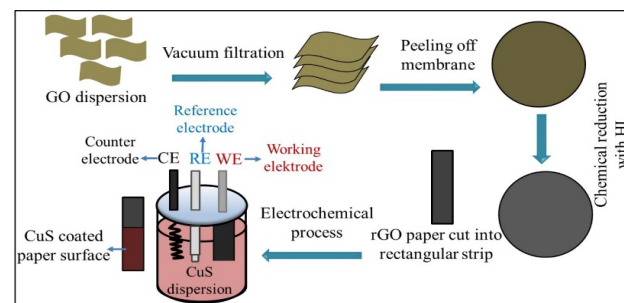


Figure 1. Schematic of the fabrication of flexible CuS/rGO composite paper.

SEM technique was used for the morphological characterization of the prepared rGO and CuS/rGO paper electrodes. SEM image of rGO paper was presented in Fig. 2a. The characteristic wrinkled structure of graphene was observed on the surface of

rGO paper (Fig. 2.a). SEM images of CuS/rGO paper (Fig. 2b and c) exhibited that porous ball-like structures of CuS covered the surface of rGO paper.

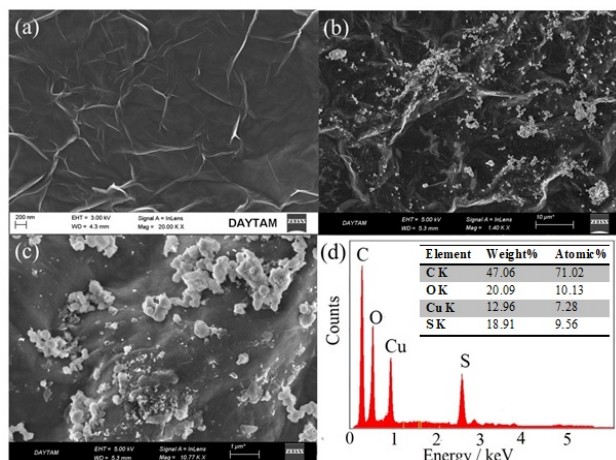


Figure 2. SEM images of (a) rGO paper, (b, c) CuS/rGO composite paper at different magnifications. (d) EDS spectra of CuS/rGO composite paper.

EDS profiles for surface structure analysis of CuS/rGO composite paper was shown in Fig. 2d. It was found that CuS/rGO composite paper contains C (47.06%), O (20.09%), Cu (12.96%), and S (18.91%), which attributed that the composite structure was successfully fabricated.

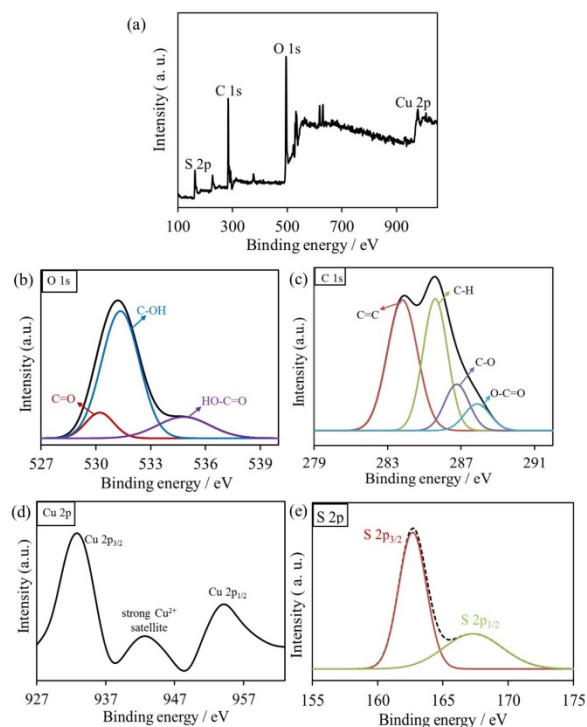


Figure 3. XPS spectra of CuS/rGO composite paper material: (a) survey, (b) O 1s, (c) C 1s, (d) Cu 2p, and (e) S 2p.

XPS method was used for chemical structure analysis of as-prepared flexible CuS/rGO composite paper. In the XPS spectrum (Fig. 3a) demonstrated

that the CuS/rGO composite paper contains 45.37% C, 23.26% O, 17.25% Cu, and 20.35% S atoms. The O 1s peak of CuS/rGO exhibited the presence of three types of O bonds, C=O, C-OH, and HO-C=O (Fig. 3b), while C 1s peak of CuS/rGO showed four types of C bonds, C=C, C-H, C-O, and O-C=O (Fig. 3c). In the Cu 2p high-resolution XPS spectrum of CuS/rGO (Fig. 3d), the binding energy peaks at 932 and 950 eV are corresponding to Cu 2p_{3/2} and Cu 2p_{1/2} [24]. S 2p_{3/2} and S 2p_{1/2} peaks formed at 162.5 eV and 167.5 eV attributed to the presence of S at the CuS/rGO paper (Fig. 3e) [16]. XPS results displayed that the designed composite paper was successfully fabricated in the desired composition.

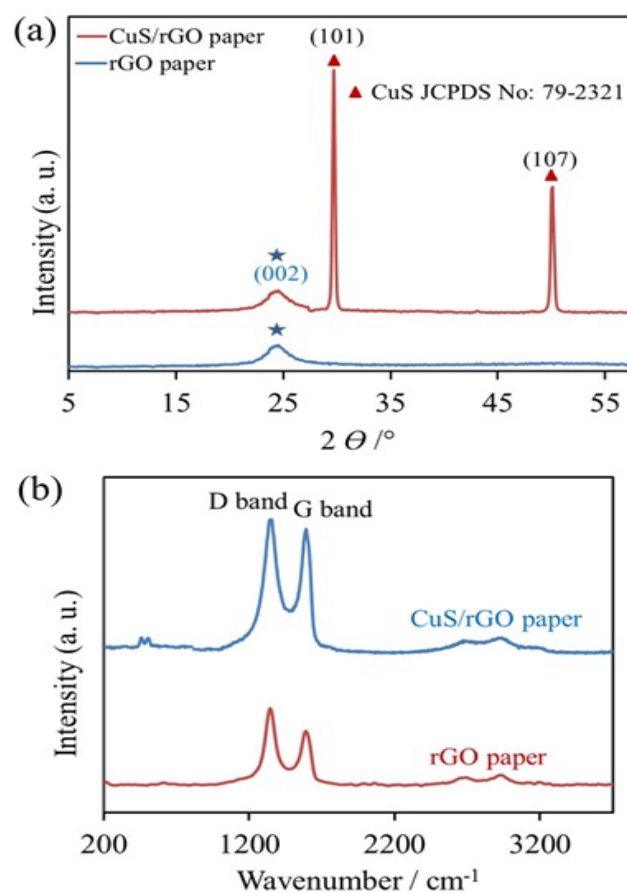


Figure 4. (a) XRD patterns, (b) Raman spectra of rGO, and CuS/rGO papers.

The XRD spectra of rGO and CuS/rGO papers were shown in Fig. 4a. In the XRD data of rGO paper, the diffraction peak (JCPDS 41-1487) corresponding to the characteristic rGO (002) crystal structure was observed at 24.8°. XRD spectrum of CuS/rGO paper, showed the peaks at about 29.5°, and 49.8°, corresponding to (101) and (107) structure of CuS, respectively (JCPDS 79-2321) [25]. Observation of the diffraction peaks of both rGO and CuS for CuS/rGO composite paper exhibited that this flexible composite paper was successfully prepared.

The Raman spectra of rGO and CuS/rGO composite papers were presented in Fig. 4b. Raman spectra of rGO paper showed G band, corresponding to E_{2g} geometry of two dimensional hexagonal C=C sp² structure, at 1610 cm⁻¹. Besides, the D band was observed at 1365 cm⁻¹, resulting from defects of the graphene layers [4,9]. Raman spectrum of CuS/rGO composite paper showed peaks corresponding to CuS structure in the range of 200 to 1000 cm⁻¹ in addition to D and G bands, attributing that the CuS structure deposited onto the rGO paper surface. The intensity of the D and G bands (I_D/I_G) is used to determine the surface defects of graphene-based papers. The I_D/I_G ratios of the rGO and CuS/rGO composite papers were calculated as 1.72 and 1.32, respectively. The I_D/I_G ratio of CuS/rGO composite paper is lower than that of rGO paper. This may be attributed to the deposition of CuS structures on surface defects of rGO paper.

CV measurements in the electrochemical solution containing Fe(CN)₆^{3-/4-} redox pair were carried out to compare the electrochemical performance of rGO paper and CuS/rGO (Fig. 5a). ΔE_p values of rGO and CuS/rGO papers were observed as 360 and 150 mV, respectively. In Fig. 5a, the peak current density of the CuS/rGO composite paper was about 2 times higher than the rGO paper. These results displayed that self-standing and flexible CuS/rGO composite paper has a quite high electrochemical activity.

For electrochemical studies, EIS is used to investigate the electron transfer mechanism in the electrode-solution interface. The Nyquist curves for rGO paper and CuS/rGO composite paper were presented in Fig. 5b. As seen from Fig.5b inset, the Nyquist curves were fitted according to the electrical circuit and electron transfer resistances (R_p) at the interface were determined for the paper electrodes. The smaller the R_p value, the easier the electron-transfer. R_p values of rGO paper and CuS/rGO composite paper were calculated as 125 and 78 Ω , respectively. The results showed that electron transfer over CuS/rGO composite paper would be easier compared to rGO paper. The cut-off point of the Z'_{re} -axis in the Nyquist curves is related to the solution resistance (R_u). R_u values of both paper electrodes were found to be very close since the same electrochemical solution was used [26].

Fig. 6 demonstrated the N₂ adsorption-desorption isotherms and pore size distributions of rGO and CuS/rGO papers at 77K. It was determined that due to CuS structure on rGO surface, CuS/rGO exhibited a typical hysteresis cycle, which was resulting in a large number of mesoporous pore [27,28]. Isotherm

curves were compatible with the Brunauer-Emmett-Teller (BET) model.

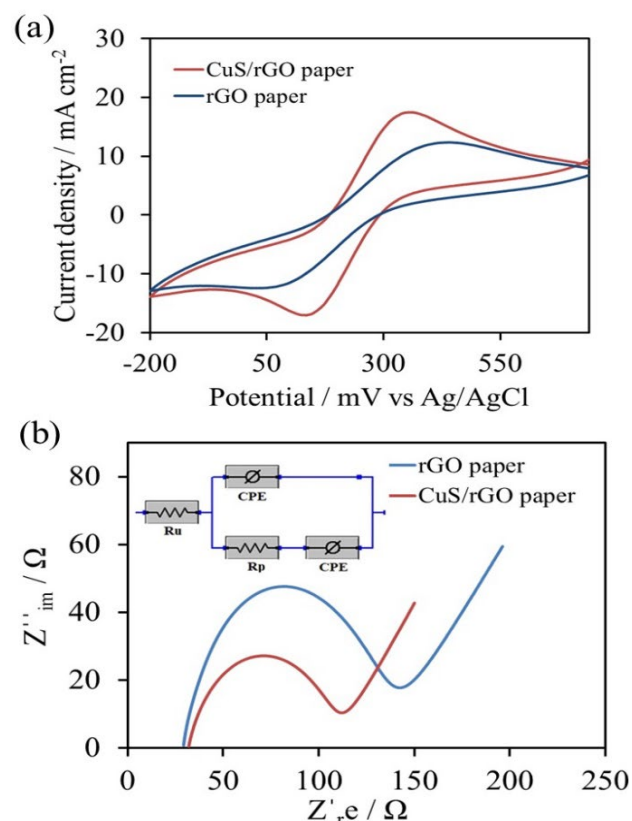


Figure 5. (a) CV curves, (b) Nyquist plots of rGO and CuS/rGO paper electrodes in a solution containing 10 mM K₃Fe(CN)₆, 10 mM K₄Fe(CN)₆ and 0.1 M KNO₃. Inset: The equivalent circuit model. Frequency range: 0.1-10⁵ Hz.

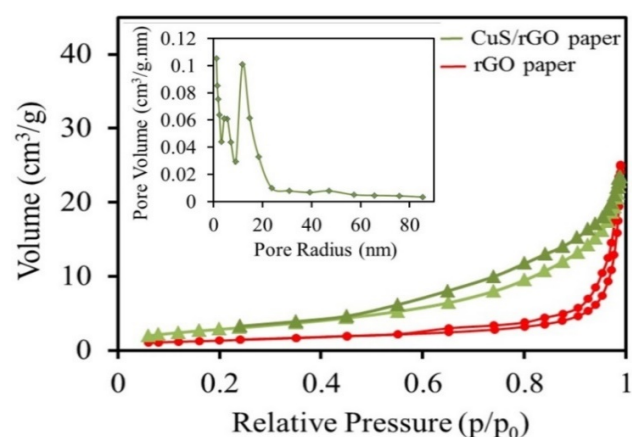


Figure 6. (a) N₂ adsorption-desorption isotherms of rGO, and CuS/rGO papers. Inset: BJH pore size distributions of CuS/rGO paper.

BET surface areas and Barrett-Joyner-Halenda (BJH) pore size distributions [29] of rGO and CuS/rGO papers were shown in Table 1. The surface area of the rGO and CuS/rGO papers was calculated as 40 and 62 m² g⁻¹, respectively (Table 1). Table 1 exhibited that CuS/rGO composite paper has a large surface area and high pore size, compared to rGO paper. This

porous property of flexible composite paper can provide an effective surface area for electrochemical studies [30].

Table 1. BET surface area and average pore size of rGO and CuS/rGO papers.

Paper Electrodes	BET surface area (m ² g ⁻¹)	Average pore radius (nm)
rGO	39	3-9
CuS/rGO	61	4-16

4. Conclusion

CuS structures synthesized through a simple hydrothermal method were electrochemically coated onto the surface of rGO paper to prepare flexible and self-standing CuS/rGO composite paper. In the morphological characterization of CuS/rGO composite paper, it was observed that the surface of the rGO was covered homogeneously with ball-like CuS structures. Structural analysis performed with XPS, XRD, and Raman techniques showed that the flexible CuS/rGO paper electrode was successfully prepared in the desired composition. Electrochemical studies demonstrated that the electrochemical activity of flexible CuS/rGO composite paper is high enough to be used as an electrode.

References

- [1] K.D. Kiranşan, E. Topçu, M. Alanyaloğlu, Surface-confined electropolymerization of pyronin Y in the graphene composite paper structure for the amperometric determination of dopamine, *J Appl Polym Sci*, 134, 2017, 45139.
- [2] K. Dağcı, M. Alanyaloğlu, Preparation of free-standing and flexible graphene/Ag nanoparticles/poly(pyronin Y) hybrid paper electrode for amperometric determination of nitrite, *ACS Appl Mater Inter*, 8, 2016, 2713-2722.
- [3] E. Topçu, K. Dağcı, M. Alanyaloğlu, Free-standing graphene/poly(methylene blue)/AgNPs composite paper for electrochemical sensing of NADH, *Electroanal*, 28, 2016, 2058-2069.
- [4] E. Topçu, K.D. Kiranşan, Flexible and free-standing PtNLS-MoS₂/reduced graphene oxide composite paper: A High-performance rolled paper catalyst for hydrogen evolution reaction, *ChemistrySelect*, 3, 2018, 5941-5949.
- [5] K.D. Kiranşan, E. Topçu, Graphene paper with sharp-edged nanorods of Fe-CuMOF as an excellent electrode for the simultaneous detection of catechol and resorcinol, *Electroanal*, 31, 2019, 2518-2529.
- [6] K. Dağcı Kiranşan, M. Aksoy, E. Topçu, Flexible and freestanding catalase-Fe₃O₄/reduced graphene oxide paper: Enzymatic hydrogen peroxide sensor applications, *Mater Res Bull*, 106, 2018, 57-65.
- [7] J.K. Lee, K.B. Smith, C.M. Hayner, H.H. Kung, Silicon nanoparticles-graphene paper composites for Li ion battery anodes, *Chem Commun*, 46, 2010, 2025-2027.
- [8] E. Topçu, K. Dağcı Kiranşan, Flexible gold nanoparticles/rGO and thin film/rGO papers: novel electrocatalysts for hydrogen evolution reaction, *J Chem Technol Biot*, 94, 2019, 3895-3904.
- [9] K. Chi, Z. Zhang, J. Xi, Y. Huang, F. Xiao, S. Wang, Y. Liu, Freestanding graphene paper supported three-dimensional porous graphene-polyaniline nanocomposite synthesized by inkjet printing and in flexible all-solid-state supercapacitor, *ACS Appl Mater Inter*, 6, 2014, 16312-16319.
- [10] K.D. Kiranşan, E. Topçu, Free-standing and flexible MoS₂/rGO paper electrode for amperometric detection of folic acid, *Electroanal*, 30, 2018, 810-818.
- [11] E. Topçu, K.D. Kiranşan, Electrochemical simultaneous sensing of melatonin and ascorbic acid at a novel flexible B-RGO composite paper electrode, *Diam Relat Mater*, 105, 2020, 107811.
- [12] E. Topçu, Three-dimensional, free-standing, and flexible cobalt-based metal-organic frameworks/graphene composite paper: A novel electrochemical sensor for determination of resorcinol, *Mater Res Bull*, 121, 2020, 110629.
- [13] K.D. Kiranşan, Preparation and characterization of highly flexible, free-standing, three-dimensional and rough NiMOF/rGO composite paper electrode for determination of catechol, *ChemistrySelect*, 4, 2019, 6488-6495.
- [14] H. Li, Y. Wang, J. Huang, Y. Zhang, J. Zhao, Microwave-assisted synthesis of CuS/graphene composite for enhanced lithium storage properties, *Electrochim Acta*, 225, 2017, 443-451.
- [15] J.T. Cao, Y.X. Dong, Y. Ma, B. Wang, S.H. Ma, Y.M. Liu, A ternary CdS@Au-g-C₃N₄ heterojunction-based photoelectrochemical immunosensor for prostate specific antigen detection using graphene oxide-CuS as tags for signal amplification, *Anal Chim Acta*, 1106, 2020, 183-190.
- [16] A.A. Sagade, R. Sharma, Copper sulphide (Cu₂S) as an ammonia gas sensor working at room temperature, *Sensor Actuat B Chem*, 133, 2008, 135-143.
- [17] N. Sreelekha, K. Subramanyam, D. Amaranatha Reddy, G. Murali, S. Ramu, K. Rahul Varma, R.P. Vijayalakshmi, Structural, optical, magnetic and photocatalytic properties of Co doped CuS diluted magnetic semiconductor nanoparticles, *Appl Surf Sci*, 378, 2016, 330-340.
- [18] M. Saranya, C. Santhosh, R. Ramachandran, P. Kollu, P. Saravanan, M. Vinoba, S.K. Jeong, A.N. Grace, Hydrothermal growth of CuS nanostructures and its photocatalytic properties, *Powder Technol*, 252, 2014, 25-32.
- [19] X.S. Hu, Y. Shen, L.H. Xu, L.M. Wang, Y.J. Xing, Preparation of flower-like CuS by solvothermal method and its photodegradation and UV protection, *J Alloy Compd*, 674, 2016, 289-294.
- [20] W. Wang, L. Ao, Synthesis and characterization of crystalline CuS nanorods prepared via a room temperature one-step, solid-state route, *Mater Chem Phys*, 109, 2008, 77-81.
- [21] Y. Zhao, H. Pan, Y. Lou, X. Qiu, J. Zhu, C. Burda, Plasmonic Cu_{2-x}S nanocrystals: Optical and structural properties of copper-deficient copper (I) sulfides, *J Am Chem Soc*, 131, 2009, 4253-4261.
- [22] N.I. Kovtyukhova, Layer-by-layer assembly of ultrathin composite films from micron-sized graphite oxide sheets and polycations, *Chem Mater*, 11, 1999, 771-778.
- [23] N. Loudhaief, M. Ben Salem, H. Labiadh, M. Zouaoui, Electrical properties and fluctuation induced conductivity studies of Bi-based superconductors added by CuS nanoparticles synthesized through the aqueous route, *Mater Chem Phys*, 242, 2020, 122464.
- [24] S. Iqbal, A. Bahadur, A. Saeed, K. Zhou, M. Shoaib, M. Waqas, Electrochemical performance of 2D polyaniline anchored CuS/Graphene nano-active composite as anode material for lithium-ion battery, *J Colloid Interf Sci*, 502, 2017, 16-23.

- [25] T. Hurma, S. Kose, XRD Raman analysis and optical properties of CuS nanostructured film, *Optik (Stuttg)*, 127, 2016, 6000-6006.
- [26] D. Song, J. Xia, F. Zhang, S. Bi, W. Xiang, Z. Wang, L. Xia, Y. Xia, Y. Li, L. Xia, Multiwall carbon nanotubes-poly(diallyldimethylammonium chloride)-graphene hybrid composite film for simultaneous determination of catechol and hydroquinone, *Sensor Actuat B Chem*, 206, 2015, 111-118.
- [27] D. Jiang, Q. Xu, S. Meng, C. Xia, M. Chen, Construction of cobalt sulfide/graphitic carbon nitride hybrid nanosheet composites for high performance supercapacitor electrodes, *J Alloy Compd*, 706, 2017, 41-47.
- [28] J. Luo, J. Lai, N. Zhang, Y. Liu, R. Liu, X. Liu, Tannic acid induced self-assembly of three-dimensional graphene with good adsorption and antibacterial properties, *ACS Sustain Chem Eng*, 4, 2016, 1404-1413.
- [29] Y. Li, H. Bin Zhang, L. Zhang, B. Shen, W. Zhai, Z.Z. Yu, W. Zheng, One-pot sintering strategy for efficient fabrication of high-performance and multifunctional graphene foams, *ACS Appl Mater Inter*, 9, 2017, 13323-13330.
- [30] J. Sha, C. Gao, S.K. Lee, Y. Li, N. Zhao, J.M. Tour, Preparation of three-dimensional graphene foams using powder metallurgy templates, *ACS Nano*, 10, 2016, 1411-1416.